Functional cone rescue by RdCVF protein in a dominant model of retinitis pigmentosa.

Ying Yang, Saddek Mohand-Saïd, Aude Danan, Manuel Simonutti, Valérie Fontaine, Emmanuelle Clérin, Serge Picaud, Thierry Léveillard, José-Alain Sahel

Functional cone rescue by RdCVF protein in a dominant model of retinitis pigmentosa

Ying Yang[1,3*], Saddek Mohand-Said[1,2,3*], Aude Danan[2], Manuel Simonutti[1,3], Valérie Fontaine[1,3], Emmanuelle Clerin[1,3], Serge Picaud[1,3], Thierry Léveillard[1,3], José-Alain Sahel[1,2,3,4, 5]

1. Université Pierre et Marie Curie-Paris6, UMR-S 592, Paris, F-75012 France
2. Centre Hospitalier National d'Ophtalmologie des Quinze-Vingts, service du Pr Sahel, Paris, F-75012
3. Institut de la Vision, INSERM, U592, Paris, F-75012
4. Institute of Ophthalmology, University College of London, UK
5. Fondation Ophtalmologique A. de Rothschild, Paris, F-75019.

Correspondence should be addressed to T.L. (thierry.leveillard@inserm.fr)

Tel: 331 53 46 25 48

Fax 331 53 46 25 02

Short title: RdCVF injection in the P23H RP model

[*] These authors contributed equally to this work.

GenBank EU861029

ABSTRACT

In retinitis pigmentosa (RP), a majority of causative mutations affect genes solely expressed in rods; however cone degeneration inevitably follows rod cell loss. Following transplantation and *in vitro* studies we demonstrated the role of photoreceptor cell paracrine interactions and identified a Rod-derived-Cone Viability Factor, RdCVF, which increases cone survival. In order to establish the clinical relevance of such mechanism, we assessed the functional benefit afforded by the injection of this factor in a frequent type of rhodopsin mutation, the P23H rat. In this model of autosomal dominant RP, RdCVF expression decreases in parallel with primary rod degeneration, which is followed by cone loss. RdCVF protein injections induced an increase in cone cell number and, more importantly, a further increase in the corresponding electroretinogram. These results indicate that RdCVF can not only rescue cones but also preserve significantly their function. Interestingly, the higher amplitude of the functional versus the survival effect of RdCVF on cones indicates that RdCVF is acting more directly on cone function. The demonstration at the functional level of the therapeutic potential of RdCVF in the most frequent of dominant RP mutations paves the way towards the use of RdCVF for preserving central vision in many RP patients.

Functional cone rescue by RdCVF protein in a dominant model of retinitis pigmentosa

Ying Yang[1,3*], Saddek Mohand-Said[1,2,3*], Aude Danan[2], Manuel Simonutti[1,3], Valérie Fontaine[1,3], Emmanuelle Clerin[1,3], Serge Picaud[1,3], Thierry Léveillard[1,3], José-Alain Sahel[1,2,3,4, 5]

1. Université Pierre et Marie Curie-Paris6, UMR-S 592, Paris, F-75012 France
2. Centre Hospitalier National d'Ophtalmologie des Quinze-Vingts, service du Pr Sahel, Paris, F-75012
3. Institut de la Vision, INSERM, U592, Paris, F-75012
4. Institute of Ophthalmology, University College of London, UK
5. Fondation Ophtalmologique A. de Rothschild, Paris, F-75019.

Correspondence should be addressed to T.L. (thierry.leveillard@inserm.fr)

Tel: 331 53 46 25 48

Fax 331 53 46 25 02

Short title: RdCVF injection in the P23H RP model

[*] These authors contributed equally to this work.

GenBank EU861029

ABSTRACT

In retinitis pigmentosa (RP), a majority of causative mutations affect genes solely expressed in rods; however cone degeneration inevitably follows rod cell loss. Following transplantation and *in vitro* studies we demonstrated the role of photoreceptor cell paracrine interactions and identified a Rod-derived-Cone Viability Factor, RdCVF, which increases cone survival. In order to establish the clinical relevance of such mechanism, we assessed the functional benefit afforded by the injection of this factor in a frequent type of rhodopsin mutation, the P23H rat. In this model of autosomal dominant RP, RdCVF expression decreases in parallel with primary rod degeneration, which is followed by cone loss. RdCVF protein injections induced an increase in cone cell number and, more importantly, a further increase in the corresponding electroretinogram. These results indicate that RdCVF can not only rescue cones but also preserve significantly their function. Interestingly, the higher amplitude of the functional versus the survival effect of RdCVF on cones indicates that RdCVF is acting more directly on cone function. The demonstration at the functional level of the therapeutic potential of RdCVF in the most frequent of dominant RP mutations paves the way towards the use of RdCVF for preserving central vision in many RP patients.

INTRODUCTION

Retinitis Pigmentosa is a photoreceptor degenerative disease caused by various mutations affecting many different genes [1]. Whereas most causative genes are selectively expressed in rod photoreceptors [2,3], a sequential rod-cone photoreceptor loss is observed in humans as well as in animal models, which is reflected by the designation of this condition as a rod-cone dystrophy. In clinical terms, while the loss of the rod photoreceptors leads to dark-adapted vision loss, the most feared visual impairment is the consequence of the secondary cone photoreceptor loss, as this cell population is necessary for diurnal vision, including photopic visual field, visual acuity, color perception and contrast sensitivity [4]. Therefore the development of therapeutic strategies targeting the mechanisms underlying the secondary cone cell death in RP represents a very promising approach. This could be applied in a wide range of mutations expressed in rods, even at late stages of the disease as it has been shown that vision may remain substantial even when 95% of cones have been lost [5]. In other words, keeping the functional cones alive may prevent up to 1.5 million people worldwide becoming blind [6].

We previously studied the rod-cone cellular interactions and proposed, following photoreceptor transplantation studies in the *rd1* mouse that the secondary cone degeneration could be significantly diminished by a surviving signal, released by rods or requiring their presence [7,8]. We subsequently demonstrated *in vitro* that these rod-cone interactions are mediated by secreted proteins [9,10]. A systematic expression cloning strategy then enabled us to isolate a Rod-derived Cone Viability Factor (RdCVF) encoded by the *Nxnl1 (Txnl6)* gene [11]. This factor is able to rescue cone photoreceptors in the *rd1* mouse. We could not assess the functionality of the rescued cones as, at the age of RdCVF injection, i.e. once rods

had degenerated, the *rd1* mouse no longer presented a measurable electroretinogram (ERG) [12].

In order to validate the therapeutic interest of RdCVF in RP, we performed this study aimed at demonstrating its functional benefit. We have selected a larger animal model carrying a prevalent RP gene mutation, the transgenic rhodopsin P23H mutant rat. This corresponds to the most frequent autosomal dominant human RP mutation observed in 12% of autosomal dominant patients in the United States [1] while the *rd1* mouse is affected by a mutation in the rod specific beta subunit gene of the cGMP-dependent phosphodiesterase 6 [13], responsible for less than 5% of autosomal-recessive RP in humans.

We characterized the course of cone photoreceptor degeneration in the P23H rat at both electrophysiological and histological levels and assessed these parameters following RdCVF protein injection. The study provides the first evidence for a functional rescue of cone photoreceptor following RdCVF administration in an animal model of RP. Moreover, our results support a possible role of RdCVF in the maintenance of the functionality of cones [14].

The clinical significance of such functional rescue cannot be underestimated, in view of the reported discrepancy between the morphological and functional effects on photoreceptor cells of another neuroprotective agent [15], ciliary neurotrophic factor (CNTF), currently in phase II clinical trials [16].

RESULTS

Secondary cone loss follows rod cell death in the P23H transgenic rats

In the P23H rat model, a transgene corresponding to the P23H mutated mouse rhodopsin gene is expressed under the control of the rhodopsin promoter, and thus expressed selectively by rod photoreceptors [17]. Histology sections show progressive thinning and loss of outer segments and outer nuclear layer between 2 to 8 months corresponding to rod loss in the heterozygotous P23H rats as previously published [18, result not shown]. **Figure 1a** shows the decrease of cone density, estimated by stereological cell counting from 3 to 9 months. By six months of age most rods have degenerated while only 41% of cones have been lost with a further 28% loss of cones between 6 and 9 months.

Functional assessment performed by ERG recordings shows a loss of scotopic and photopic function during photoreceptor degeneration (**Figs. 1b-e**). The average amplitude of the scotopic ERG B-wave was reduced by 75% between 2 and 4 months (from 268 μV to 66 μV; **Fig. 1d** and **Table 1**), and was further reduced by up to 89% at 9 months (29 μV), while the photopic ERG B-wave amplitude decreased by, respectively 56% (77 μV versus 34 μV) and 77% (18 μV) during the same periods. Loss of cone function was further confirmed by flicker ERG (**Fig. 1e**).

Thus, as observed for the *rd1* mouse [9,11,19], rod degeneration, triggered here by the expression of the mutant protein in rod cells, is followed by a secondary loss of cones through a non-cell-autonomous mechanism. The sequential degeneration of rods and cones in the heterozygotous P23H model makes it therefore an appropriate model for the assessment of cone rescue strategies.

Decreased RdCVF expression correlates with rod loss in the P23H rat model

We then investigated the expression of RdCVF, a trophic factor expressed in a rod-dependent manner in the mouse [11]. Mouse RdCVF-L protein sequence (Uniprot: Q8VC33) was used to identify the rat RdCVF sequence (**Figs. 2a,b**). As for the mouse *Nxnl1* (*Txnl6*) and *Nxnl2* genes, different forms of RdCVF mRNAs were identified resulting most likely from alternative splicing [20]. Using RT-PCR, RdCVF-Total expression (short and long forms) was found to be expressed in the neural retina but not in the retinal pigment epithelium of the rat (**Fig. 3a**). Using specific primers we quantified by real-time RT-PCR the expression of RdCVF and RdCVF-L mRNAs. The steady state level of RdCVF total mRNAs increases gradually during the period from PN10 to PN30 in wild-type retinas, however in P23H retinas it reaches a maximum expression at PN20 (lower than that in wild-type at this stage) then decreases by PN30 (**Fig. 3b**). β-actin was used as an internal control and the relative expression of RdCVF was 27% and 7% in the Sprague-Dawley (SD) and Pro23His rat retinas respectively, they represent only 1.1% and 0.8% in the P23H rat retina at 6 months of age, after rod photoreceptors have been lost. Quantitative RT-PCR also shows a rod-dependent expression matching that of rod arrestin (result not shown). To confirm the rod-dependent expression of RdCVF, we analyzed by western blotting the expression of RdCVF during the course of rod photoreceptor maturation and degeneration in the P23H rat retina using RdCVF-N rabbit polyclonal antibodies [11]. The intensity of the band corresponding to RdCVF-L is shown to increase during the maturation of the retina between PN10 and 3 months in the wild-type rat but up to 2 months in the P23H rat (**Fig. 3c**). For the P23H retina the RdCVF-L expression lags behind that of normal retina and starts to decrease from 2.5 to 4 months, the period of rod loss. The reduced RdCVF-L immunoreactivity in wild-type retina is most likely reflecting a loading difference as seen on the top panel. A non-specific band migrating at the position of the short isoform of RdCVF interferes with quantitative analysis. However in spite of this, a decrease in expression may still be seen at 4 months. We next localized RdCVF

expression in the retina by immunohistochemistry using the same antibodies. The expression of the *Nxnl1* (*Txnl6*) gene products could be detected in the SD retina at PN10 with increasing expression to 3 months at which stage stable expression is achieved up to 5 months of age (**Fig. 3d**). This expression pattern matches that of rhodopsin in the rod outer segments at the same period. Also, in P23H rat retina, RdCVF labeling is localized to the photoreceptor outer segments, but decreases as the segments shorten (3 to 5 months).

Subretinal injections of RdCVF protein delay both cone cell death and photopic visual loss

RdCVF protein (109 aa) was chemically synthesized (>90% purity) and refolded (**Fig. 4a**). The activity of the synthesized protein was measured using an *in vitro* cone-enriched culture system. As, when compared to a fusion protein purified after expression in E. coli, the synthesized protein showed equivalent protective activity and was of higher purity, the latter was consequently used for injection (**Fig. 4b**, result not shown). Three injections of the synthesized polypeptide (1.5 µg) were performed at different time point (separately at the age of 6, 7, 8 month) in the sub-retinal space of the P23H rats. PBS was injected as negative control (SM). The cone density in the RdCVF injected eyes (1790±231 c/mm²) at 9 months of age, one month after the last subretinal injection, was increased by 19% compared to the sham controls (1498±141 c/mm²) and by 20% compared to the contralateral controls (1497±133 c/mm², **Fig. 4c**). Moreover, the surviving cones were distributed in the whole retina, and not only localized in the areas of injection (data not shown).

We also examined the effect of RdCVF injection on cone function by measuring the photopic electroretinogram. An example of the photopic ERG response following RdCVF injections is provided in **Figure 4d**. RdCVF injections were found to limit the decrease in photopic ERG observed between 4 and 9 months (see **Fig. 1d**). The amplitude of the photopic

ERG B-wave in RdCVF injected eyes (**Fig. 4e**, 43±24 μV) was 115% and 126% higher respectively than in the contralateral control eyes (20±13 μV) and sham operated eyes (19±11 μV). The differences observed after RdCVF injection were statistically significant ($p<0.01$). The scotopic responses however did not show any significant difference between all the groups examined. Thus, RdCVF protein administration is providing a selective protection of cone photoreceptor function.

The observation of a larger functional effect, as compared to cytoprotection (**Fig. 4e** versus **4c**) led us to analyze the morphology of photoreceptors. Several reports document that changes in the length and morphology of outer segments occur prior to cell death and that they relate to functional alterations [21,22]. The cones of wild-type retina (**Fig. 5a**) displayed longer outer segments than those of P23H rat retina at 9 months of age (**Fig. 5b**). The region surrounded by a white line with higher magnification corresponds to the diameter of the tip areas of cone outer segments on flat-mounted retinas. The tip areas of cone outer segments in P23H rat retina (**Fig. 5b**) were larger than in wild-type retina (**Fig. 5a**). Such shortening of cone outer segments and the enlargement of the tip of cone outer segments on flat-mounted retinas imply that the P23H cones are dysmorphic which relates to dysfunction even before dying. As the enlargement of the tip of cone outer segments appears as a proper marker of this event, we compared the size of the tip area of cone outer segments from RdCVF treated, untreated control and sham retinas. We scanned the flat-mounted RdCVF-injected retinas (9 months of age) stained by PNA lectin using an automated acquisition system (**Figs. 5c,d**). The measure was performed for five retinas of each group in 40 fields at 0.2 mm from the optic nerve in all directions. The areas of 5 to 25 cones in each field were measured in a masked test. In **Figure 5i** and **Table 2**, the tip areas of cone outer segments in the RdCVF treated retinas (21±7 μm^2) are 38% and 34% smaller respectively than in the untreated control retinas (34±10 μm^2) and sham retinas (32±9 μm^2). These differences after RdCVF injection were

statistically significant (both, $p<0.001$). The correlation between cone outer segment morphology and cone function is even more apparent when the data of **Figure 5i** are plotted with those of **Figure 4e**, the data points then align in a strength lane with a regression R of 0.8939. To get more details on the morphology of the cones, the images acquired from 9 focus plans were reconstructed in 3D using Metamorph software and converted into 2D using the optimal focus as shown in **Figure 5e** and **5f**. The surface of the selected cells is e- 6.6 µm², f- 4.5 µm². The hollow area inside is e- 1.9 µm², f- 0.8 µm². These data imply that the total surface of the selected cell and the inner hole area are smaller in RdCVF treated P23H retina than in untreated control P23H retina. Furthermore, we scanned the cone cells from both the RdCVF treated and non-treated retinas by using confocal microscope and we observed smaller, ellipse tip area (white star) and longer outer segment in the RdCVF treated retina (double arrow, **Fig. 5h**), than in the non-treated retina (**Fig. 5g**). Therefore RdCVF injection induced a morphological pattern resembling that observed in normal cones or prior to rod degeneration. This observation that the morphology of cone outer segments after RdCVF injection might be correlated with the increased response to light stimuli is scored in **Figure 4e**.

DISCUSSION

The importance of rod/cone interactions for cone survival was suggested subsequent to the identification of the first causal mutations in retinitis pigmentosa [23,24]. Indeed, despite the fact that these causal genes are often solely expressed in rods, the degeneration of cones is nonetheless triggered [19,25,26]. The production of animal models with the selective ablation of rod photoreceptors confirmed this rod dependence of cone survival [27]. The rod-dependence of cone survival is also supported by the experiments *in vitro* [28] and by the

studies of transgenic mice and mutant zebrafish [29-31], suggesting cell-to-cell interactions in photoreceptor degeneration. Photoreceptor transplantation in the *rd1* mouse provided evidence that rod presence is required for cone survival [8]. The demonstration of the rod/cone dependence was directly provided by co-culture experiments [9]. These results were obtained by transplantation and co-culture in the *rd1* mouse. Yet, this model has important limitations as rods degenerate before the complete differentiation of the photoreceptors. Moreover, cone degeneration is observed at an age when no cone ERG signal can be recorded [12]. We have here used a rat model of RP in another species, the P23H transgenic rat, widely acknowledged as relevant for preclinical studies.

RdCVF was isolated for its effect on cone survival using embryonic chick cone cultures [11]. In the P23H rat retina, by 6 months of age most rods have degenerated and lost most of their function (**Fig. 1, b** and **d**). The effect of the injections of RdCVF protein from 6 to 8 months indicates that this factor induces cone survival directly but does not act indirectly by stimulating rod survival, as most rods have already degenerated at the time of treatment. Similarly, this trophic effect appears independent from the mechanisms of rod degeneration and thus of the causal mutation when the mutated gene is only expressed in rods. Indeed, although photoreceptors undergo apoptosis in both the *rd1* mouse [32] and the P23H rat [1], this apoptosis is attributed to the cGMP toxicity [33] and Ca^{2+} fluxes in the *rd1* mouse [34,35] whereas, by contrast, in the P23H model, it is reported to result from a gain of function due to the toxicity of the mutated rhodopsin [36]. Therefore, RdCVF is very likely to act directly on cone survival but not to interfere with the mechanisms of rod degeneration. Furthermore, we also observed that cone photoreceptor distribution extended through the whole retina, but not localized in some areas, showing such an extent of the rescue may relate to the multiple subretinal injections and the spread achieved.

Importantly, RdCVF induces also a functional rescue validating thereby the potential of this trophic factor for therapeutic applications. On account of the large variance observed in ERGs between rats at the same age, we performed a paired student T-test for statistical analysis from each rat between the treated and untreated control eyes. On average, the cone numbers were increased by 20% and photopic ERG B-wave amplitudes were increased by 115%. In addition, by comparison between these P23H rats and wild type rats (201±63 μV), we observed that photopic ERG B-wave amplitudes from the RdCVF protein injected eyes reached 43% of wild type, in contrast to only 10% in the non-injected eyes. The more evident improvement in the ERG measurement compared to overall cone number may indicate that the ratio of functional cones with respect to surviving cones was increased by RdCVF protein injection, implying that RdCVF has a direct effect on cone function. Moreover, ERG B-wave amplitude was about 30 μV when RdCVF injections were started (6 months), then it raised to over 40 μV ($P<0.01$) after repeated treatment, implying that this improvement might be due to changes in photoreceptor activity, changes in bipolar or horizontal cell function to photoreceptor input, or synaptic connectivity from the surviving cone. We suggest that it might be caused by changes of cone photoreceptor outer segments which were observed both in the photoreceptor transplanted and injected retinas. Recently it has been shown that exposing the P23H rat for one week to photopic ambient light results in the reduction of the cone B-wave amplitude by 57%, an effect that could not be explained by photoreceptor loss as the cone cell density was unchanged, but was associated with the shortening of cone outer segments [37]. In addition the cone outer segments were swollen, delaminated and vesiculated. Interestingly, after 5 weeks in scotopic conditions the cone B-wave amplitude recovered to 87%, while cone outer segments were reorganized and retrieved their elongated morphology. This demonstrates the capacity of cones to recover morphologically and functionally after photo-oxidative damage and that functional changes are better correlated

with cone outer segment morphology than with cone cell density. Furthermore, it has been demonstrated that RdCVF, which is homologous to the thioredoxin family is able to protect cone cells against light irradiation [38]. Correlations between photoreceptor outer segment morphology and ERG were also demonstrated [14] reporting that CNTF treatment after 6 days caused a shortening of rod outer segments and a suppression of ERG responses, and all these changes were fully reversible after 3 weeks. They found a 62% reduction in A-wave amplitude, approximately proportional to a 46% reduction in rod outer segment length. With the loss of rod photoreceptors and resulting deficiency of RdCVF in P23H rats, even a high number of cones at the 3 month stage will nevertheless yield a lower ERG photopic B-wave recording (amplitude: 40-50 μV). This indicates that the sequence of events involves first a loss of the function followed by death of photoreceptors. It is known that cones are robust conical-shaped structures that have their cell bodies situated in a single row just below the outer limiting membrane and their inner and outer segments protruding into the subretinal space [39]. We suggest that the increase in diameter of the tip sheath is associated with the shortening of cone outer segments. Our results indirectly indicate a shortening of cone outer segments in the untreated control and sham control retinas. Importantly, they also indicate that, after RdCVF protein was injected subretinally at 6, 7 and 8 months to the P23H rats, cone outer segments of RdCVF-treated retinas presented a morphological pattern different from their untreated control and sham retinas, as the diameter of the tip sheath was significantly less enlarged, implying partial reversion of changes of cone outer segments. The outer segment is a structure filled entirely with discs of folded double membranes in which are embedded the light sensitive visual pigment molecules, thus the changes in cone outer segments of surviving cones and the improvement of ERG B-wave amplitude imply that RdCVF actually restores photopic responses in addition to slowing down cone death.

For the treatment of patients with retinitis pigmentosa, the large number of genes and, in particular, the dominant inheritance of many types of RP is a major challenge for corrective gene therapy [40]. The neuroprotective effect of FGF2 in a rat model of inherited retinal dystrophy [41] initiated the search for the most potent protective factors, an approach that would offer therapeutic potential regardless of the causal mutation. CNTF is currently being evaluated in a clinical trial [15], although the paradoxical decrease in both scotopic and photopic responses in CNTF-treated retinas [42] has led to the evaluation of other trophic factors such as glial cell derived neurotrophic factor, GDNF [12,43,44]. In addressing the secondary degeneration of cones, RdCVF administration may be used to target a pathological mechanism common to most forms of the disease. The retinal cone cells are responsible for all visual functions in normal light. Therefore, preventing their degeneration is a rational strategy in the treatment of RP patients. This objective is medically feasible since 50% cone loss does not result in significant loss of visual acuity [5] and furthermore it has been estimated that this approach may prevent up to 1.5 million people worldwide from becoming blind [6].

The present study on the P23H rat suggests that RdCVF administration may be efficient in the treatment of autosomal dominant RP due to rhodopsin mutations, which account for 30-40% of cases of human autosomal dominant RP (http://www.sph.uth.tmc.edu/Retnet/). However, photoreceptor transplantation is limited by the availability of the donors and the potential risks of contamination [45]. Also, the clinical importance of RdCVF is further suggested by the existence of RdCVF variants associated with Leber congenital amaurosis [46]. Several issues need to be addressed for us to translate our observation of functional rescue of cones by subretinal administration of RdCVF to the point of evaluation in a clinical trial. Different modes of protein delivery are indeed currently used for retinal diseases: repeated intravitreal injections as for anti-VEGF therapy in age-

related macular degeneration [47] or intravitreal implants containing engineered cells producing the proteins [48]. In both cases, the protein achieves its effect on the outer retina via delivery to the vitreous. Further studies will assess the dose response curve of RdCVF injection on cone survival in P23H rats, and evaluate whether vitreal administrations in large animal models (e.g. *rcd1* dog) could also lead to a similar functional rescue of cones. These detailed studies will address the questions of pharmacokinetics of the protein. Alternatively, RdCVF protein might be delivered using adeno-associated virus vectors [49,50]. A positive result would then open the way for RdCVF clinical validation and bring much hope to patients suffering from retinitis pigmentosa, a strategy that may be applicable to a majority of RP mutations, with relevance even at late stages of the disease when rods have already disappeared and can no longer be rescued.

MATERIALS AND METHODS

Animals

Experimental procedures adhered to the Association for Research in Vision and Ophthalmology Statement for the Use of Animals in Ophthalmology and Vision Research. Transgenic homozygous P23H rats (line 1) were kindly provided by Matthew LaVail, PhD (UCSF School of Medicine, Beckman Vision Center) and were crossed with albino Sprague-Dawley rats (SD) to obtain heterozygous animals that were used in all experiments. All animals were bred and maintained under a 12-hr light/dark cycle with a room illumination of around 15 lux at 25°C. They were housed with the authorization and supervision of the institutional Animal Care from Inserm UMR592. The animals were divided into 2 groups and operations have been performed by randomly selecting the eye to be treated. The unoperated eye from each rat was considered as natural control (contralateral controls): Group 1: Ten 3-

month-old rats for PBS subretinal injection- sham controls (SM); Group 2: Fifteen 6-month-old rats for RdCVF injection (RdCVF). ERG recordings have been performed for each animal after surgery at the age of 9 months. The animals were sacrificed with overdose anaesthesia: 2-2.5 ml ketamine 500 (Rhone Merieux, Lyon, France).

Data mining

A PSI-BLAST (Position Specific Iterative-Basic Local Alignement Search Tool) of mouse peptide was performed on EST databank from *Rattus norvegicus*. One EST (BE108041) was found to 443 pb mRNA homologous sequence in the reverse orientation (3'→5'). This EST was then localized in genomic sequence from *Rattus norvegicus* (contig: ac122603). The first exon of the gene was located between position 88325 and 88654 and the second from position 89977 to 90304. A stop codon in frame within the first intron immediately following the exon 1 predicts the production of a truncated form of the thioredoxin-like 6 protein as observed for mouse. Full length open reading frame corresponding to the rat RdCVF sequence was amplified by RT-PCR from normal rat retina and the resulting product sequenced. The 330 pb sequence is identical to that of the rat RdCVF gene mined in the genomic database (**Fig. 2a**). Rat RdCVF is 98% homologous to RdCVF from mouse (**Fig. 2b**). There are two conservative changes in amino acid sequences: V2A and D106E.

Reverse transcription-Polymerase Chain Reaction (RT-PCR) analysis

Retinal total RNA from Sprague-Dawley and transgenic rats was purified using CsCl centrifugation and reverse transcribed into cDNAs by random hexamers (pdN_6) according to standard protocols. First strand cDNA (0.25 µl) was amplified using 1 µM of sequence specific primers on a LightCycler instrument (Roche-Diagnostics, Indianapolis, IN) and with SYBR Green I (LightCycler Faststart DNA Master^{PLUS} SYBR Green I $^{®)}$, according to the

manufacturer's recommendations. Cycling conditions were as follows: initial denaturation at 95°C for 1 min, following by 40 cycles of denaturation at 95°C for 0 sec, annealing at 57°C for 5 sec, elongation at 72°C for 13 sec ended by a gradual increase (0.1 °C/sec) in temperature to 95°C. Real-time PCR efficiencies were evaluated by calculating the slope of a linear regression graph. For each experiment, crossing points were calculated by the LightCycler Data Analysis Program (LightCycler-3.5 Software). Gene expression levels were normalized with respect to that of beta-actin (β-actin). The oligonucleotides used were: 5'-AGCACAAGACGATTCTCTAAC-3', 5'-AACCCTCTCTCAAAACCAAAC-3' for RdCVF total (141 bp both short and long isoforms of the messenger RNA), 5'-TACAGAGGAGCAACAGGACCTGTTCCTCCGG-3', 5'-CGTCAACTGCCAGCGGTCGTGGTACTCAA-3' for RdCVF-L (130 bp); 5'-TTCCTGCCGTTCCATGATGACC-3', 5'-TAGCAATCCTCCTGTCTTCCCTCC-3' for RdCVF (227 bp). Results are represented in percentage compared to β-actin (296 bp) expression for which level is 100 %.

RdCVF injection

Human RdCVF polypeptide (109 amino acids) was synthesised at GeneProt (Geneva) and refolded (>90% purity). The protective effect of the RdCVF synthetic protein on cone-enriched cultures from chicken embryos was performed as previously described [11]. The injections were performed totally three times and monthly: at different post-natal month (6M, 7M and 8M). Before injections, rats were anesthetized by intramuscular injection of a mixture of ketamine (100 mg/kg) and xylazine (10 mg/kg). After anesthetizing, we exposed the superior sclera and performed a small hole by using a 10-0 needle. The induction of a local retinal detachment was checked in order to confirm the success of the subretinal injection procedure. The local retinal detachment was chosen at different locations to maximize

delivery. The microsyringe (Hamilton, 10 µl) was then gently inserted into the subretinal space, and 3 µl of synthetic RdCVF protein (concentration: 0.5 µg/µl) was injected. We used the same procedure for sham surgery where only PBS was injected to the control eye.

Cell counts and measurement of the tip areas of cone outer segments

The total numbers of PNA-labeled cones were estimated in the flat-mounted retinas by using a stereological counting approach to achieve unbiased sampling, as previously described [9]. The rat retina was subdivided into 225 fields representing a surface of 1225 µm² each. A zone of 2 mm radius centre on the optic nerve was omitted in the counting. 120-200 fields distributed throughout the remaining whole retinal surface were chosen for cone counting by using a systematic random sampling procedure: an initial random choice was made for the first measurement, and all subsequent sampling was performed at predetermined intervals throughout the retinal surface. Each field was observed and the number of cone visually counted by using a Nikon Plan 40× objective on a Nikon photomicroscope equipped with a Sony Trinitron color graphic display camera (Sony, Tokyo). The counted cone numbers and fields were cumulated automatically by the computer during the counting. The average of cone number per field was calculated in order to estimate the number of cone photoreceptors per millimeter square. The cone counts were expressed as density over the estimated retinal surface.

To measure the tip areas of cone outer segments, the flat-mounted retinas were scanned by automated acquisition system, using a Nikon Plan 40× objective. We chose 5 retinas of each group from RdCVF-treated, control and sham groups and 40 fields of each retina at 2 mm away from their optic disc in all directions. The areas of 5 to 25 cones in each field were measured in a masked analysis, by pixels (X= Y= 1 pixel = 0.3225 µm). The tip areas of PNA labelling were calculated and shown as Figure 5i. In order to get more details from the

morphology of the cones, the images built from 9 focus plans were reconstructed in 3D using Metamorph software and converted into 2D using the optimal focus.

ERG recordings

Following overnight dark adaptation, animals were prepared for recording under dim red light. After intramuscular anaesthesia with a mixture of ketamine (100mg/kg) and xylazine (10mg/kg), pupils were dilated with 0.5% tropicamide or 1% atropine and the cornea was locally anesthetized with oxbuprocaine application. Upper and lower lids were retracted to keep the eye open and proptosed. Body temperature was maintained at approximately 37°C with a heating pad. A gold loop electrode was placed on the corneal surface and maintained with lacrigel (Europhta). A stainless steel reference electrode was inserted subcutaneously on the head of the rat and a second needle electrode inserted subcutaneously in the back of the rat served to ground the signal. The light stimulus was provided by a 150 watt xenon lamp in a Ganzfeld stimulator (Multiliner Vision, Jaeger Toennies, Germany), increasing from -4 to1.4 log cd/m². Photopic cone ERGs were performed on a rod suppressing background after 5 minute light adaptation. The duration of the light stimulus was constant. Responses were amplified and filtered (1 Hz-low and 300 Hz-high cut off filters) with a 1-channel DC-/AC-amplifier. Within each treatment group, ERG recordings were performed on separate days between the treated and the control eyes in order to prevent interference of stimulations between the two eyes of the same animal. Each scotopic or photopic ERG response represents the average of five responses from a set of five flashes of stimulation. To avoid corneal opacity for the unrecorded eye during the operation, a drop of lacrigel was covered on the surface of cornea and the eyelids were closed by tweezers.

Statistical Analysis

We used the method of Smirnov to distinguish whether the data followed a normal distribution. As we selected randomly one eye of each rat for the treated sample, and another eye for the control in all the groups of experiment, all the samples for ERG and cell counts were paired to compare treated vs. control retinas in each group (cone number of each mm^2 per retina, amplitude and latency of ERG A and B waves separately). Student's t test was performed for paired series- ERG and cell counts. Analysis of variance and t test were used for unpaired series- the size of the tip areas of cone outer segments.

ACKNOWLEDGEMENTS

We thank Frédéric Chalmel and Olivier Poch for their contribution to the bioinformatic analysis (IGBMC); George Lambrou, Valérie Heidinger and Anne-Ulrike Trendelenburg for providing synthetic RdCVF protein (Novatris Ophthamics); Matthew Lavail for generously providing the P23H rat line and for his collaboration in studying cone cell degeneration in this model; Géradine Millet-Puel, Marie-Laure Niepon and Najate Aït-Ali for technical help; Thérèse Cronin for reading the manuscript and Stephane Fouquet for confocal microscope technique supports. This work was supported by Inserm, EVI-GENORET and Foundation Fighting Blindness (USA).

SUPPLEMENTARY MATERIALS

Table S1. RdCVF injection: photopic B-wave amplitudes and cone counts of the RdCVF protein injected and contralateral controls eyes from P23H rats.

Table S2. Sham operation: photopic B-wave amplitudes and cone counts of the PBS injected eyes from P23H rats.

Figure S1. Morphology of cones in the RdCVF untreated and treated retinas. Several cones scanned by confocal microscope display smaller, ellipse tip area and longer outer segment in the RdCVF treated retina (A-D), differing from larger tip area and shorter segment in the non-treated retina (E-H). Scale bar = 2 μm.

Supplementary Materials and Methods.

REFERENCES

1. Hartong, DT, Berson, EL and Dryja, TP (2006). Retinitis pigmentosa. *Lancet* **18**, 1795- 1809.

2. Rosenfeld, PJ, Cowley, GS, McGee, TL, Sandberg, MA, Berson, EL and Dryja, TP (1992). A null mutation in the rhodopsin gene causes rod photoreceptor dysfunction and autosomal recessive retinitis pigmentosa. *Nat Genet* **1**, 209-213.

3. McLaughlin, ME, Sandberg, MA, Berson, EL and Dryja, TP (1993). Recessive mutations in the gene encoding the beta-subunit of rod phosphodiesterase in patients with retinitis pigmentosa. *Nat Gene* **4**, 130-134.

4. Mangel, SC and Dowling, JE (1987). The interplexiform-horizontal cell system of the fish retina: effects of dopamine, light stimulation and time in the dark. *Pro R Soc Lond B Biol Sci* **22**, 91-121.

5. Geller, AM and Sieving, PA (1993). Assessment of foveal cone photoreceptors in Stargardt's macular dystrophy using a small dot detection task. *Vision Res* **33**, 1509-24.

6. Wright, AF (1997). A searchlight through the fog. *Nat Genet* **17**, 132-134.

7. Mohand-Said, S, Hicks, D, Dreyfus, H and Sahel, JA (2000). Selective transplantation of rods delays cone loss in a retinitis pigmentosa model. *Arch Ophthalmol* **118**, 807-811.

8. Mohand-Said, S, Hicks, D, Simonutti, M, Tran-Minh, D, Deudon-Combe, A, Dreyfus, H *et al*. (1997). Photoreceptor transplants increase host cone survival in the retinal degeneration (rd) mouse. *Ophthalmic Res* **29**, 290-297.

9. Mohand-Said, S, Deudon-Combe, A, Hicks, D, Simonutti, M, Forster, V, Fintz, A.C *et al*. (1998). Normal retina releases a diffusible factor stimulating cone

survival in the retinal degeneration mouse. *Proc Natl Acad Sci U S A* **95**, 8357-8362.

10. Fintz, AC, Audo, I, Hicks, D, Mohand-Said, S, Léveillard, T and Sahel, J (2003). Partial characterization of retina-derived cone neuroprotection in two culture models of photoreceptor degeneration. *Invest Ophthalmol Vis Sci* **44**, 818-825.

11. Léveillard, T, Mohand-Saïd, S, Lorentz, O, Hicks, D, Fintz, AC, Clérin, E *et al*. (2004). Identification and characterization of rod-derived cone viability factor. *Nat Genet* **36**, 755-759.

12. Frasson, M, Picaud, S, Léveillard, T, Simonutti, M, Mohand-Said, S, Dreyfus, H *et al*. (1999). Glial cell line-derived neurotrophic factor induces histologic and functional protection of rod photoreceptors in the rd/rd mouse. *Invest Ophthalmol Vis Sci* **40**, 2724-2734.

13. Bowes, C, Li, T, Danciger, M, Baxter, LC, Applebury, ML and Farber, DB (1990). Retinal degeneration in the rd mouse is caused by a defect in the beta subunit of rod cGMP-phosphodiesterase. *Nature* **347**, 677-680.

14. Cronin, T, Léveillard, T and Sahel, JA (2007). Retinal degenerations: from cell signaling to cell therapy; pre-clinical and clinical issues. *Curr Gene Ther* **7**, 121-129.

15. Wen, R, Song, Y, Kjellstrom, S, Tanikawa, A, Liu, Y, Li, Y *et al*. (2006). Regulation of rod phototransduction machinery by ciliary neurotrophic factor. *J Neurosci* **26**, 13523-13530.

16. Sieving, PA, Caruso, RC, Tao, W, Coleman, HR, Thompson, DJ, Fullmer, KR *et al*. (2006). Ciliary neurotrophic factor (CNTF) for human retinal degeneration: phase I trial of CNTF delivered by encapsulated cell intraocular implants. *Proc Natl Acad Sci U S A* **103**, 3896-3901.

17. Lee, D, Geller, S, Walsh, N, Valter, K, Yasumura, D, Matthes, M *et al*. (2003). Photoreceptor degeneration in Pro23His and S334ter transgenic rats. *Adv Exp Med Biol* **533**, 297-302.

18. Machida, S, Kondo, M, Jamison, JA, Khan, NW, Kononen, LT, Sugawara, T *et al*. (2000). P23H rhodopsin transgenic rat: correlation of retinal function with histopathology. *Invest Ophthalmol Vis Sci* **41**, 3200-3209.

19. Carter-Dawson, LD, LaVail, MM and Sidman, RL (1978). Differential effect of the rd mutation on rods and cones in the mouse retina. *Invest Ophthalmol Vis Sci* **17**, 489-498.

20. Chalmel, F, Léveillard, T, Jaillard, C, Lardenois, A, Berdugo, N, Morel, E *et al*. (2007). Rod-derived Cone Viability Factor-2 is a novel bifunctional-thioredoxin-like protein with therapeutic potential. *BMC Mol Biol* **8**, 74.

21. Aizawa, S, Mitamura, Y, Baba, T, Hagiwara, A, Ogata, K and Yamamoto, S (2009). Correlation between retinal sensitivity and photoreceptor inner/outer segment junction in patients with retinitis pigmentosa. *Br J Ophthalmol* **93**, 126-127.

22. Punzo, C, Kornacker, K, Cepko, CL (2009). Stimulation of the insulin/mTOR pathway delays cone death in a mouse model of retinitis pigmentosa. *Nat Neurosci* **12**, 44-52.

23. Dryja, TP, McGee, TL, Reichel, E, Hahn, LB, Cowley, GS, Yandell, DW *et al*. (1990). A point mutation of the rhodopsin gene in one form of retinitis pigmentosa. *Nature* **343**, 364-366.

24. Petters, RM, Alexander, CA, Wells, KD, Collins, EB, Sommer, JR, Blanton, MR *et al*. (1997). Genetically engineered large animal model for studying cone photoreceptor survival and degeneration in retinitis pigmentosa. *Nat Biotechnol* **15** 965-970.

25. Naash, MI, Hollyfield, JG, al-Ubaidi, MR and Baehr, W (1993). Simulation of human autosomal dominant retinitis pigmentosa in transgenic mice expressing a mutated murine opsin gene. *Proc Natl Acad Sci U S A* **90**, 5499-5503.

26. Goto, Y, Peachey, NS, Ripps, H and Naash, MI (1995). Functional abnormalities in transgenic mice expressing a mutant rhodopsin gene. *Invest Ophthalmol Vis Sci* **36**, 62-71.

27. McCall, MA, Gregg, RG, Merriman, K, Goto, Y, Peachey, NS and Stanford, LR (1996). Morphological and physiological consequences of the selective elimination of rod photoreceptors in transgenic mice. *Exp Eye Res* **63**, 35-50.

28. Hewitt, AT, Lindsey, JD, Carbott, D and Adler, R (1990). Photoreceptor survival-promoting activity in interphotoreceptor matrix preparations: characterization and partial purification. *Exp Eye Res* **50**, 79-88.

29. Huang, PC, Gaitan, AE, Hao, Y, Petters, RM and Wong, F (1993). Cellular interactions implicated in the mechanism of photoreceptor degeneration in transgenic mice expressing a mutant rhodopsin gene. *Proc Natl Acad Sci U S A* **90**, 8484-8.

30. Kedzierski, W, Bok, D and Travis, GH (1998). Non-cell-autonomous photoreceptor degeneration in rds mutant mice mosaic for expression of a rescue transgene. *J Neurosci* **18**, 4076-4082.

31. Goldsmith, P, Baier, H and Harris, WA (2003). Two zebrafish mutants, ebony and ivory, uncover benefits of neighborhood on photoreceptor survival. *J Neurobiol* **57**, 235-245.

32. Portera-Cailliau, C, Sung, CH, Nathans, J and Adler, R (1994). Apoptotic photoreceptor cell death in mouse models of retinitis pigmentosa. *Proc Natl Acad Sci U S A* **1**, 974-978.

33. Lolley, RN, Rayborn, ME, Hollyfield, JG and Farber, DB (1980). Cyclic GMP and visual cell degeneration in the inherited disorder of rd mice: a progress report. *Vision Res* **20**, 1157-1161.

34. Vallazza-Deschamps, G, Cia, D, Gong, J, Jellali, A, Duboc, A, Forster, V *et al*. (2005). Excessive activation of cyclic nucleotide-gated channels contributes to neuronal degeneration of photoreceptors. *Eur J Neurosci* **22**, 1013-1022.

35. Sanges, D, Comitato, A, Tammaro, R and Marigo, V (2006). Apoptosis in retinal degeneration involves cross-talk between apoptosis-inducing factor (AIF) and caspase-12 and is blocked by calpain inhibitors. *Proc Natl Acad Sci U S A* **14**, 17366-17371.

36. Gorbatyuk, M, Justilien, V, Liu, J, Hauswirth, WW and Lewin, AS (2007). Suppression of mouse rhodopsin expression in vivo by AAV mediated siRNA delivery. *Vision Res* **47**, 1202-1208.

37. Chrysostomou, V, Stone, J, Stowe, S, Barnett, NL and Valter, K (2008). The status of cones in the rhodopsin mutant P23H-3 retina: light-regulated damage and repair in parallel with rods. *Invest Ophthalmol Vis Sci* **49**, 1116-1125.

38. Wang, XW, Tan, BZ, Sun, M, Ho, B and Ding JL (2008). Thioredoxin-like 6 protects retinal cell line from photooxidative damage by upregulating NF-kappaB activity. *Free Radic Biol Med* **45**, 336-344

39. Steinberg, RH, Fisher, SK and Anderson, DH (1980). Disc morphogenesis in vertebrate photoreceptors. *J Comp Neurol* **190**, 501-508.

40. Delyfer, MN, Léveillard, T, Mohand-Said, S, Hicks, D, Picaud, S and Sahel, JA (2004). Inherited retinal degenerations: therapeutic prospects. *Biol Cell* **96**, 261-269.

41. Faktorovich, EG, Steinberg, RH, Yasumura, D, Matthes, MT and LaVail, MM (1990). Photoreceptor degeneration in inherited retinal dystrophy delayed by basic fibroblast growth factor. *Nature* **347**, 83-86.

42. Rhee, KD, Ruiz, A, Duncan, JL, Hauswirth, WW, LaVail, MM, Bok, D *et al*. (2007). Molecular and cellular alterations induced by sustained expression of ciliary neurotrophic factor in a mouse model of retinitis pigmentosa. *Invest Ophthalmol Vis Sci* **48**, 1389-1400.

43. McGee Sanftner, LH, Abel, H, Hauswirth, WW and Flannery, JG (2001). Glial cell line derived neurotrophic factor delays photoreceptor degeneration in a transgenic rat model of retinitis pigmentosa. *Mol Ther* **4**, 622-629.

44. Buch, PK, Maclaren, RE, Duran, Y, Balaggan, KS, MacNeil, A, Schlichtenbrede, FC *et al*. (2006). In contrast to AAV-mediated Cntf expression, AAV-mediated Gdnf expression enhances gene replacement therapy in rodent models of retinal degeneration. *Mol Ther* **14**, 700-709.

45. Chong, NH and Bird, AC (1999). Management of inherited outer retinal dystrophies: present and future. *Br J Ophthalmol* **83**, 120-122.

46. Hanein, S, Perrault, I, Gerber, S, Dollfus, H, Dufier, JL, Feingold, J *et al*. (2006). Disease-associated variants of the rod-derived cone viability factor (RdCVF) in Leber congenital amaurosis. Rod-derived cone viability variants in LCA. *Adv Exp Med Biol* **572**, 9-14.

47. Rosenfeld, PJ, Brown, DM, Heier, JS, Boyer, DS, Kaiser, PK, Chung, CY *et al*. (2006). Ranibizumab for neovascular age-related macular degeneration. *N Engl J Med* **5**, 1419-1431.

48. Tao, W (2006). Application of encapsulated cell technology for retinal degenerative diseases. *Expert Opin Biol Ther* **6**, 717-726.

49. Maguire, AM, Simonelli, F, Pierce, EA, Pugh, ENJr, Mingozzi, F, Bennicelli, J *et al*. (2008). Safety and Efficacy of Gene Transfer for Leber's Congenital Amaurosis. *N Engl J Med* **358**, 2240-2248.

50. Bainbridge, JW, Smith, AJ, Barker, SS, Robbie, S, Henderson, R, Balaggan, K *et al*. (2008). Effect of Gene Therapy on Visual Function in Leber's Congenital Amaurosis. *N Engl J Med* **358**, 2231-2239.

Table 1. Scotopic and photopic ERG amplitude and latency of Sprague Dawley and P23H rats.

	Scotopic b wave (1logcds/m²)		Photopic b wave (1.4 logcds/m²)	
	Latency (ms)	Amplitude (μV)	Latency (ms)	Amplitude (μV)
Sprague Dawley (N=12)	81±8	913±165	68±12	201±63
P23H 2 months	85±13	268±34 CI: 248~287	67±16	77±19 CI: 66~88
P23H 4 months	96±12	66±16 CI: 57~75	96±13	34±9 CI: 28~41
P23H 6 months	98±12	45±19 CI: 35~54	96±11	28±16 CI: 20~36
P23H 9 months	105±20	29±16 CI: 23~35	105±23	18±13 CI: 15~22

CI: 95% confidence interval, which is an interval estimate of a population parameter. Here are shown only the confidence intervals of P23H rat ERG scotopic and photopic B wave amplitude from 2 to 9 months.

Table 2. The size of the tip areas of cone outer segments.

Number of the retinas	RdCVF (μm²)	Control (μm²)	Sham (μm²)
1	22.15±6.93	31.03±8.56	35.05±8.31
2	20.72±6.68	31.39±10.28	31.73±10.28
3	25.04±8.25	34.02±9.11	31.02±8.17
4	19.29±6.49	30.77±8.17	29.22±7.68
5	22.16±6.74	39.67±10.43	35.92±10.93
Average of 5 retinas	21.45±7.21	33.56±9.95	31.81±9.11

FIGURE LEGENDS

Figure 1

Photoreceptor degeneration of P23H mutant rats. (**a**) Cone counts, 3 months: 4913±128 c/mm², 6 months: 2894±259 c/mm², 9 months: 1527±166 c/mm². (**b**) Mixed responses to single flashes of intensity (1 log cds/m²) in dark adapted condition of P23H rats at different ages. (**c**) Under photopic adaptation, responses to single flashes (1.4 log cds/m²) of P23H rats at different ages. (**d**) Curved lines display scotopic (black) and photopic (red) B-wave amplitude reduction with age. (**e**) Under photopic adaptation, rapid responses of P23H rat retinas to flashes (0.477 log cds/m²) at 10, 20, 30 Hz, showing progressive decreases in Flicker ERG with age.

Figure 2

RdCVF-S (short form) sequence of Rattus norvegicus. (**a**) RdCVF-S nucleotide sequenced and its deduced amino acids sequence. The epitope of the polyclonal antibodies used is underlined. In bold, a difference in nucleotide sequence between the two species. (**b**) Alignment of rat with mouse RdCVF protein. In bold are highlighted the amino acid differences between the two polypeptides.

Figure 3

Decreased expression of RdCVF in the P23H retina. (**a**) RT-PCR products of RdCVF-total mRNA amplification from wild-type. β-actin mRNA by RPE was shown as a positive control. The expression of RdCVF and RdCVF-L mRNA was tested by RT-PCR with specific primer sets. NR: neural retina. RPE: retinal pigment epithelium. H_2O: no RNA. (**b**) Expression of RdCVF total (RdCVF and RdCVF-L) mRNAs in P23H and wild-type (WT) retinas from PN10 to PN30. Results are expressed as a fold difference to expression in the RPE (Retinal

Pigment Epithelium) took as reference. Indeed, expression of retinal genes is very low in the RPE and could be considered as background noise. (**c**) Expression of RdCVF protein according to retinal degeneration. Western blotting of protein extracted (40 µg/lane) from P23H and wild-type (wt) retinas (at PN10, 30, 40 and month 2, 2.5, 3, 4) were probed with anti-RdCVF-N and anti-alpha-tubulin antibodies. Bands at 50 kDa (β-tubulin) and at 30 kDa correspond to RdCVF-L protein. β-tubulin was used to control equal quantities which were loaded in each lane. (**d**) Immunocytochemical localisation of RdCVF (red), rhodopsin (green) and DAPI (blue) for wild-type (WT) and P23H rats with retinal development. OS: outer segments, IS: inner segments, ONL: outer nuclear layer, OPL: outer plexiform layer, INL: inner nuclear layer.

Figure 4

Effect of RdCVF peptide injection to P23H retinas at 9 months of age. (**a**) Coomassie staing of the synthetic RdCVF protein. (**b**) Protective effect of the RdCVF synthetic protein of the cone-enriched cultures from chicken embryos. (**c**) Percentage of changing cone number by normalization from the injected and corresponding control eyes. (SM: 98%, RdCVF: 120%, **P<0.001). (**d**) Comparison of photopic ERG average of 5 single flashes from a P23H rat (B-wave amplitude: control eye- 36 µV, operated eye- 83 µV). (**e**) Amplitudes of photopic ERG B-wave of the treated and control eyes in each group. CO: control eye, SM: sham control eye, RdCVF: RdCVF injected eye.

Figure 5

Analysis of the morphology of the cones. (**a** and **b**) Immunolabeling of PNA lectin (green) and Rho-4D2 antibody (red) in wild type retina (**a**, WT) and P23H retina (**b**) at 9 months. The cones in the enlarged images (rectangles in the right side of both images **a** and **b**) shown by

white arrow head demonstrate the cone outer segments are longer and the tip areas of cone outer segments (white ellipse line) are smaller in wild-type retina than in P23H retina. Scale bar = 25 μm. (**c-f**) By automated acquisition system with a marker of PNA lectin displays the tip areas of cone outer segments are bigger in the control (**c**) than in the RdCVF treated retina (**d**). Scale bar = 12.5 μm. **e**, **f**: Using Metamorph software, the cones shown by white arrow head in Figure **5e** and **5f** were reconstructed in 2D by the optimal focus. The surface of the selected cells is **e**- 6.6 μm², **f**- 4.5 μm². The inner hole area (white star) of the selected cells is **e**- 1.9 μm², **f**- 0.8 μm². (**g** and **h**) Two cones scanned by confocal microscope display smaller, ellipse tip area (white star) and longer outer segment in the RdCVF treated retina (double arrow, **h**), but not in the non-treated retina (**g**). Scale bar = 2 μm. (**i**) Comparison of the tip areas of cone outer segments by PNA labeling in control, sham, and RdCVF injected retinas. This was performed by analysing an average of 432 cones per retina.

ABBREVIATIONS

β-actin, beta-actin; CNTF, ciliary neurotrophic factor; CO, control; ERG, electroretinogram; PNA, peanut agglutinin lectin; RdCVF, Rod-derived-Cone Viability Factor; Rho-4D2, anti-rhodopsin antibody; RP, retinitis pigmentosa; SD, Sprague-Dawley; SM, sham operation control.

Figure 1

Click here to download high resolution image

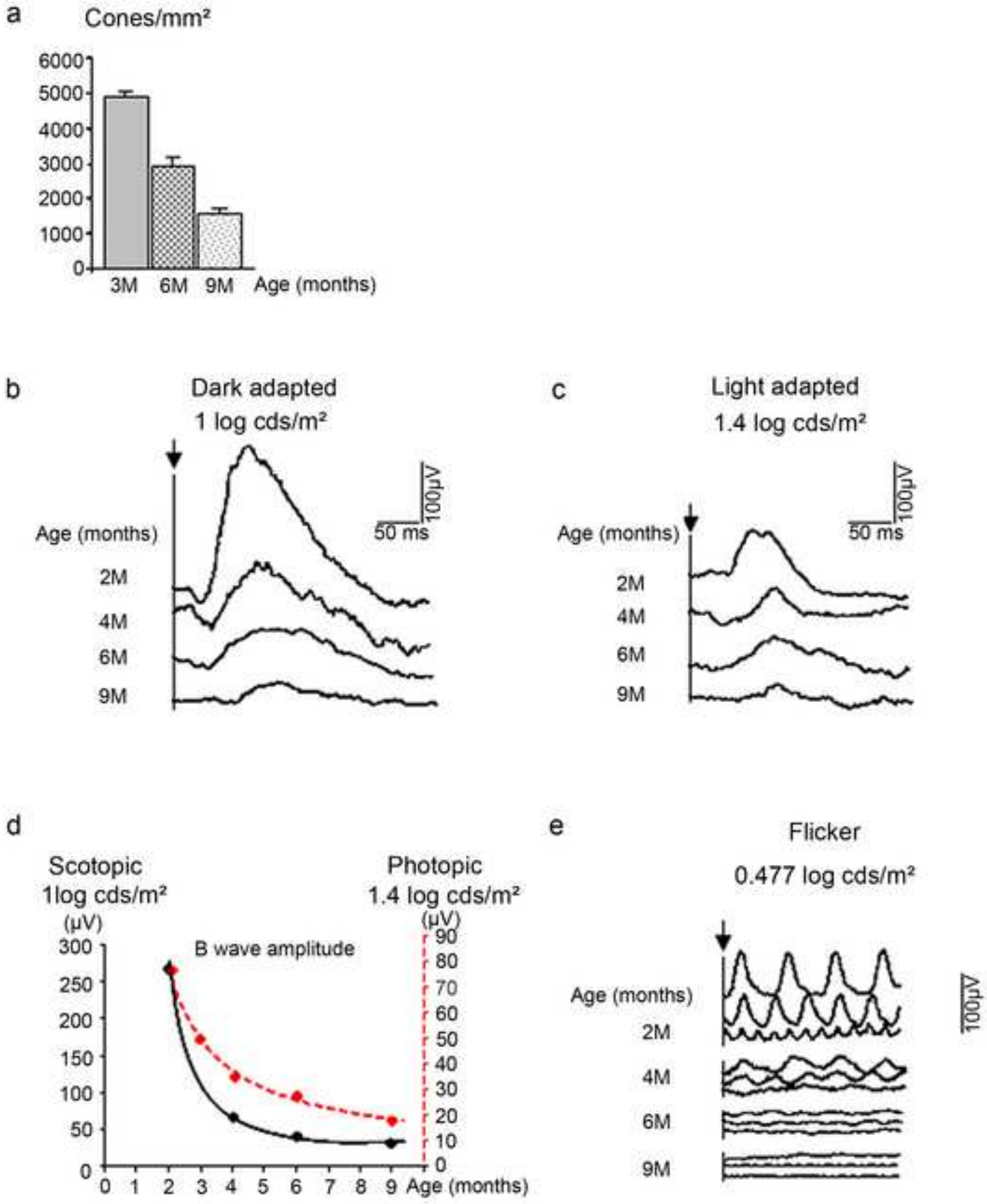

Figure 2

Click here to download high resolution image

Figure 3

Click here to download high resolution image

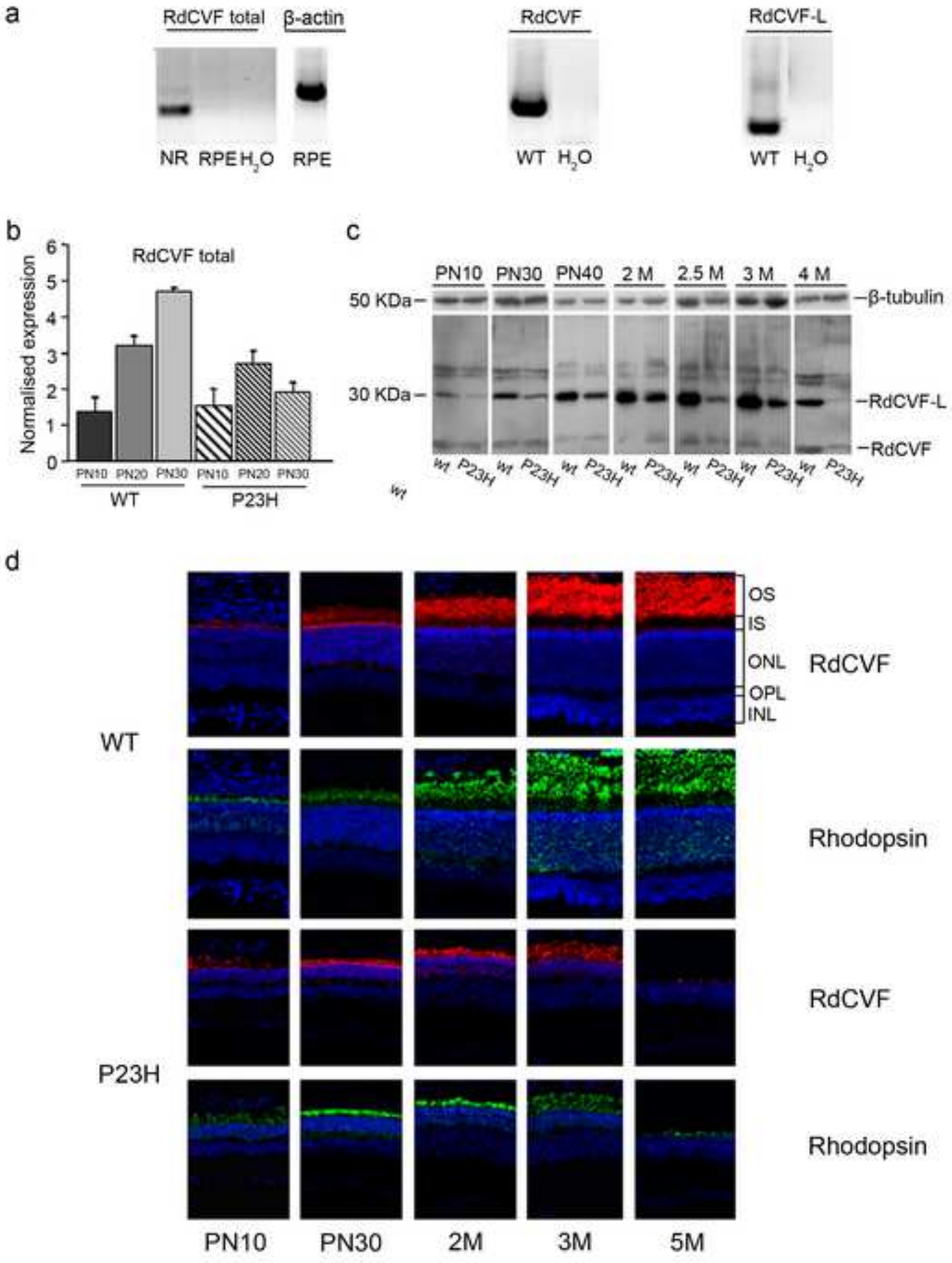

Figure 4

Click here to download high resolution image

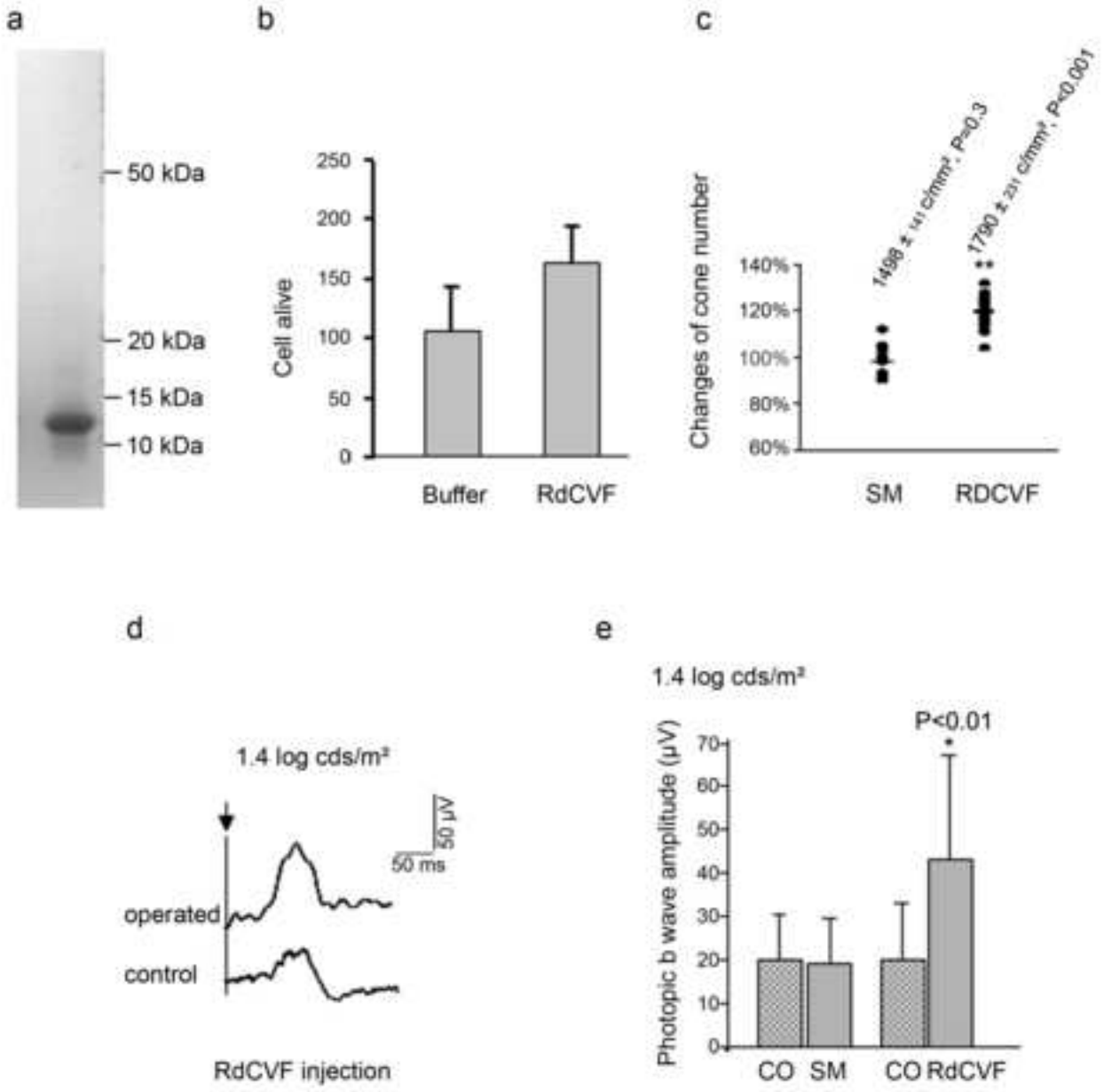

Figure 5

Click here to download high resolution image

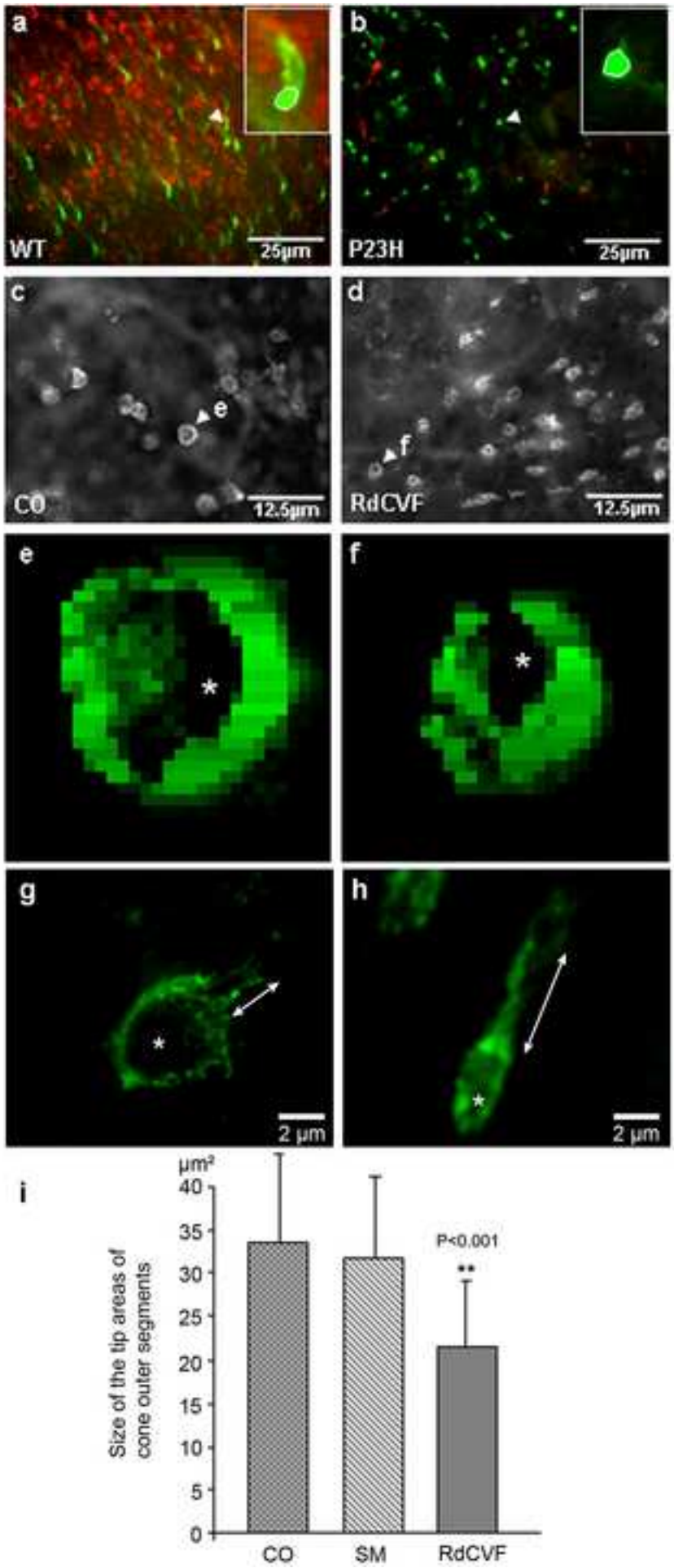

Supplementary Materials and Methods

Immunohistochemistry

For cryosection, after enucleation, a small hole performed from the limbus of the cornea allows better penetration of the fixative liquid in all the tissues. The eyes were immersed at 4°C overnight in 4% paraformaldehyde in Phosphate buffered saline 0.01M, pH 7.4. The tissues were incubated successively in 10%, 20% sucrose at 4°C for cryoprotection and embedded in OCT. For total neural retinas, the eyes were enucleated quickly and immersed in PBS. The anterior segment, lens, and vitreous body were removed. The neural retinas were initially fixed in 4% paraformaldehyde 2 hrs at 4°C, rinsed by PBS 3 times (5 minutes each), then as vertical sections (7 μm), permeabilized for 5 minutes in PBS containing 0.1% Triton X-100, and incubated in PBS containing 1% BSA, 0.1% Tween-20 for 30 minutes at room temperature. (FITC)-conjugated peanut agglutinin (PNA, 1: 50) lectin from arachis hypogae and anti-rhodopsin antibody (Rho-4D2, 1: 250) were incubated overnight at 4°C to label respectively cone and rod photoreceptor cells. For rhodopsin antibody, after washing, sectioned tissues or total neural retinas were incubated with a secondary antibody: goat anti-mouse IgG conjugated to either Alexa TM 594 or 488 at 1: 500 for 1 hr. The nuclear marker DAPI was added to the incubation solution only for sectioned tissues which were ultimately mounted with Flurosave reagent (Calbiochem, San Diego, CA). Sections (7 μm) were counterstained by hematoxylin and eosin to assess retinal morphology and thickness of the photoreceptor layer. Unsectioned total neural retinas, were flat mounted in gel (Biomeda, Foster city, CA), with the photoreceptor layer facing up.

Western Blot Analysis

Retinas from postnatal day (PN) 10, 30, 40 and month 2, 2.5, 3, 4.5 were dissected and homogenized by sonication in a lysis buffer containing 50 mM Tris-HCl pH 7.5, 1 mM EDTA, 1 mM dithiothreitol, 1% Triton X-100, 1 mM phenylmethylsulphonyl fluoride, 50 µg/ml N-tosyl-L-lysine-chloromethyl ketone, 1 mM sodium fluoride and 1 mM sodium orthovanadate and protease inhibitors cocktail. Protein concentrations were measured by Bradford's assay. 40 µg of proteins were loaded on a 12% SDS-PAGE and transferred onto nitrocellulose. The membrane was saturated with PBS 1 X, 0.05% Tween-20, 5% nonfat dry milk overnight at 4°C and then incubated for 3 hours at room temperature with 0.1 µg/ml affinity-purified anti-RdCVF rabbit polyclonal antibodies. After washing, the membrane was incubated with peroxidase-conjugated goat anti-rabbit secondary antibody (1: 15000; Jackson ImmunoResearch Laboratories, Hamburg, Germany) for one hour at room temperature. Antibody binding was revealed by Enhanced Chemiluminescence system and hyperfilm-ECL X-ray film (Amersham Pharmacia Biotech). To check that equal quantities of protein extract were loaded in each lane, antibody-removal was achieved with 100 mM mercaptoethanol, 2% SDS, 620.5 mM Tris-HCl pH 6.7, the membrane was then washed, saturated and subsequently reprobed with monoclonal anti-alpha-tubulin antibody (1: 1000; T5168, Sigma, Saint Louis, MO).

Supplemental Table S1

Click here to download Supplemental Table: Supplementary Table S1.doc

Supplementary Table S1:

RdCVF injection

Number of rats	Photopic ERG B-wave amplitude (μV) **operated eye**	Photopic ERG B-wave amplitude (μV) **control eye**	Photopic ERG B wave latency (ms) **operated eye**	Photopic ERG B wave latency (ms) **control eye**	Cone counts (number /mm^2) **operated eye**	Cone counts (number /mm^2) **control eye**
1	82.9	36.0	90.0	94.8	1486	1322
2	53.9	3.9	135.6	97.2	2049	1633
3	56.5	46.6	93.6	116.4	1673	1469
4	40.2	31.5	126.0	86.4	1918	1616
5	75.2	24.2	91.2	102.0	1869	1543
6	55.5	5.3	141.6	98.4	1878	1559
7	20.2	19.4	90.0	93.6	1453	1265
8	38.3	35.5	80.4	79.2	1584	1257
9	25.4	20.4	84.0	116.4	2253	1486
10	26.7	4.6	110.4	55.2	2155	1682
11	86.8	20.5	86.4	94.8	1731	1518
12	24.0	15.9	88.8	98.4	1722	1486
13	25.5	22.4	96.0	96.0	1714	1551
14	28.3	2.9	79.2	81.6	1706	1641
15	7.9	14.8	121.2	54.0	1657	1420

Supplemental Table S2

Click here to download Supplemental Table: Supplementary Table S2.doc

Supplementary Table S2:

Sham operation

Number of rats	Photopic ERG B-wave amplitude (μV) **operated eye**	Photopic ERG B wave latency (ms) **operated eye**	Cone counts (number /mm^2) **operated eye**
1	7.5	128.4	1320
2	13.0	108.0	1380
3	26.2	97.2	1550
4	22.4	122.4	1507
5	37.1	94.8	1678
6	22.7	99.6	1400
7	20.9	104.1	1367
8	8.5	93.6	1649
9	27.3	91.2	1707
10	2.5	98.4	1423

Supplemental Figure S1
Click here to download high resolution image

Supplementary figure 1